

Summary of the 2014/2015 Asian Winter Monsoon

This report summarizes the characteristics of the surface climate and atmospheric/oceanographic considerations related to the Asian winter monsoon for 2014/2015.

Note: The Japanese 55-year Reanalysis (JRA-55¹; Kobayashi et al. 2015) atmospheric circulation data and COBE-SST (JMA 2006) sea surface temperature (SST) data were used for this investigation. The outgoing longwave radiation (OLR) data referenced to infer tropical convective activity were originally provided by NOAA. The base period for the normal is 1981 – 2010. The term “anomaly” as used in this report refers to deviation from the normal.

1. Surface climate conditions

1.1 Overview of Asia

In boreal winter 2014/2015, temperatures were above or near normal in many parts of East Asia and in Siberia, and were below normal from seas south of Japan to the Philippines and around eastern India. Very low temperatures were recorded around Japan in December, and very high temperatures were recorded from Central Siberia to eastern China in January (Figure 1.1 and 2.7).

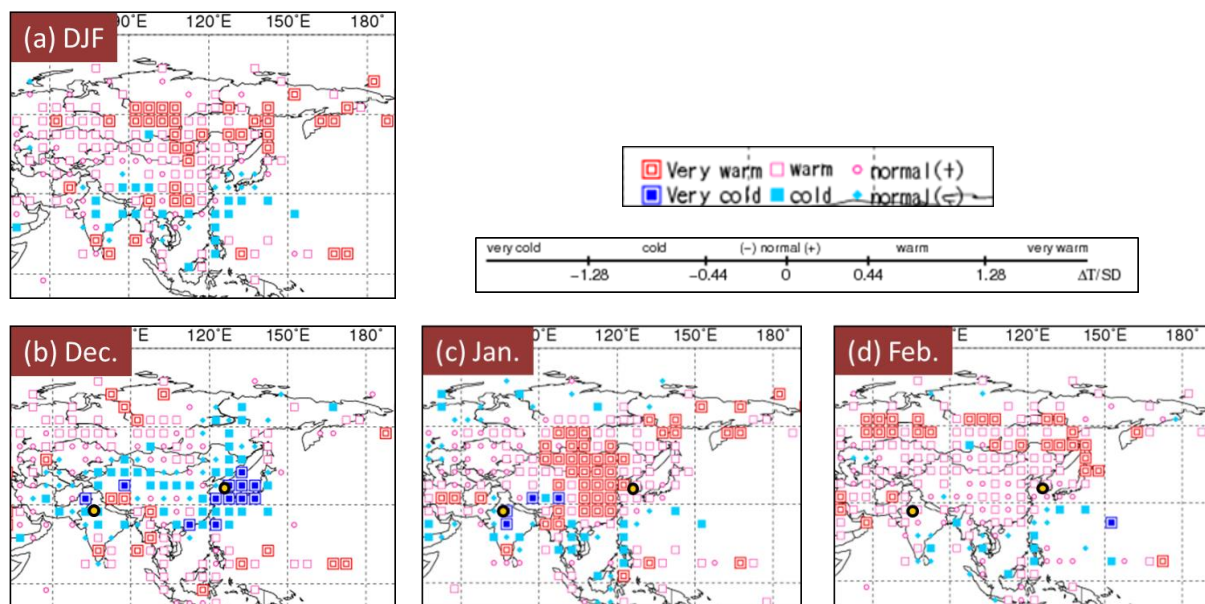


Figure 1.1 (a) Three-month mean temperature anomalies for December 2014 – February 2015, and monthly mean temperature anomalies for (b) December 2014, (c) January 2015 and (d) February 2015

Categories are defined by the three-month/monthly mean temperature anomaly divided by its standard deviation and averaged in $5^\circ \times 5^\circ$ grid boxes. The thresholds of each category are -1.28, -0.44, 0, +0.44 and +1.28. Standard deviations were calculated from 1981 – 2010 statistics. Areas over land without graphical marks are those where observation data are insufficient or where normal data are unavailable. Orange-colored circles in figures (b) - (d) indicate locations of New Delhi (India) and Incheon (Republic of Korea). Daily temperature data for both cities are shown in Figure 1.3.

¹ http://jra.kishou.go.jp/JRA-55/index_en.html

Figure 1.2 shows extreme climate events occurring between December 2014 and February 2015. In December, extremely low temperatures were observed in northwestern China and from Pakistan to northwestern India. Extremely heavy precipitation amounts were observed around Japan and from central Indonesia to Sri Lanka. In January, extremely high temperatures were seen in the eastern part of Eastern Siberia and from the southern part of Central Siberia to eastern China. Extremely heavy precipitation amounts were observed around the Indochina Peninsula. In February, extremely high temperatures were observed around the southern part of Eastern Siberia, and extremely heavy precipitation amounts were observed around the southern part of Central Asia.

Figure 1.3 shows a time-series representation of daily temperatures at New Delhi in India and Incheon in Republic of Korea during winter 2014/2015. Daily mean temperatures were below normal on many days from mid-December to late January, and were above normal in early December and the second half of February at New Delhi. Daily mean temperatures were below normal on many days in December, and were above normal on many days in January and February at Incheon.

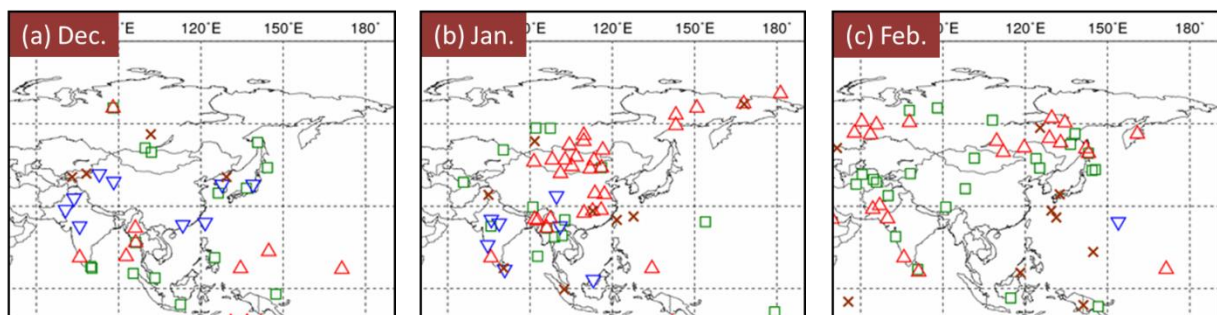


Figure 1.2 Extreme climate events for (a) December 2014, (b) January 2015 and (c) February 2015

△ Extremely high temperature ($\Delta T/SD > 1.83$) □ Extremely heavy precipitation ($Rd = 6$)
 ▽ Extremely low temperature ($\Delta T/SD < -1.83$) × Extremely light precipitation ($Rd = 0$)
 ΔT , SD and Rd indicate temperature anomaly, standard deviation and quintile, respectively.

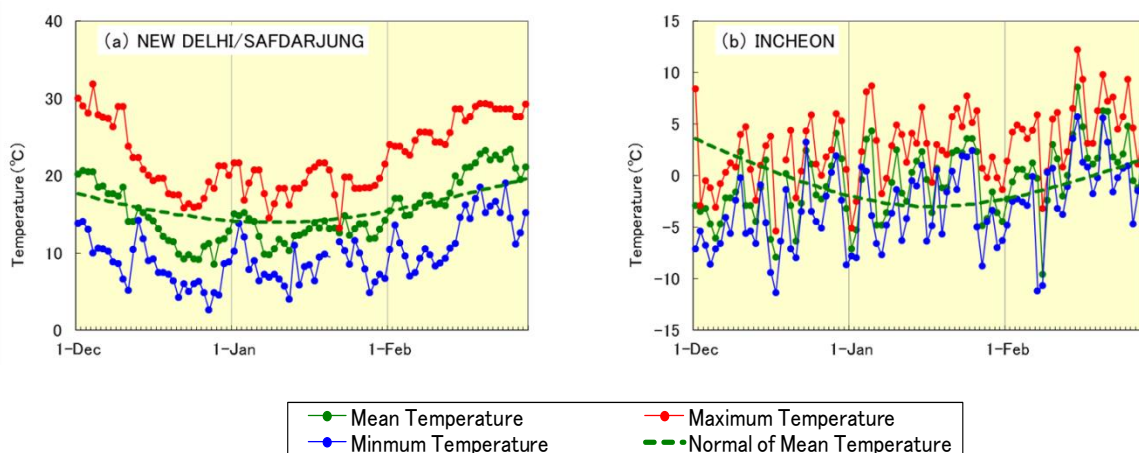


Figure 1.3 Time series of daily maximum, mean and minimum temperatures (°C) at New Delhi in India and Incheon in Republic of Korea from 1 December 2014 to 28 February 2015 (based on SYNOP reports)

2. Characteristic atmospheric circulation and oceanographic conditions

2.1 Conditions in the tropics and Asian Winter Monsoon

In winter 2014/2015, sea surface temperatures (SSTs) were above normal in the western-to-central equatorial Pacific and below normal in the western equatorial Indian Ocean (Figure 2.1). An active convection phase of the Madden-Julian Oscillation was seen propagating eastward from the Indian Ocean to the western Pacific from late November to early December, followed by another active phase from late December to early January, both with enhanced amplitude (Figure 2.2). Convective activity averaged over the three months from December to February was enhanced from the Maritime Continent to the western equatorial Pacific (Figure 2.3 (a)).

In December 2014, large-scale divergence anomalies in the upper troposphere were pronounced over the eastern equatorial Indian Ocean (Figure 2.3 (b)). These convection anomalies are thought to have served as a heating source in association with the development of a pattern with anticyclonic circulation anomalies centered over South China and cyclonic circulation anomalies seen around Japan (Figure 2.4 (b)), which contributed to enhanced cold air flow into East Asia. This is corroborated by a resemblance between the actual pattern of anticyclone-cyclone anomalies and the steady response seen in a linear baroclinic model (LBM) experiment forced with observed heating anomalies (Figure 2.5). It is therefore probable that the low temperatures experienced in East Asia during December were related to the enhanced convective activity observed over the eastern Indian Ocean.

In January 2015, anticyclonic circulation anomalies in the upper troposphere centered over East Asia (Figure 2.4 (c)) and the weaker-than-normal Siberian High (Figure 2.8 (c)) were related to the higher-than-normal temperatures recorded around eastern China (Figure 1.1 (c)). Upstream of these anticyclonic anomalies, cyclonic circulation anomalies were centered over the northern part of the Bay of Bengal, presumably in association with heavy precipitation experienced over parts of the Indochina Peninsula (Figure 1.2 (b)). These anomalies constituted a wave train pattern propagating eastward from the Middle East along the subtropical jet stream.

In February 2015, the subtropical jet stream over the area from South Asia to East Asia shifted southward of its normal position as indicated in Figure 2.4 (d) in association with suppressed convective activity around Indonesia.

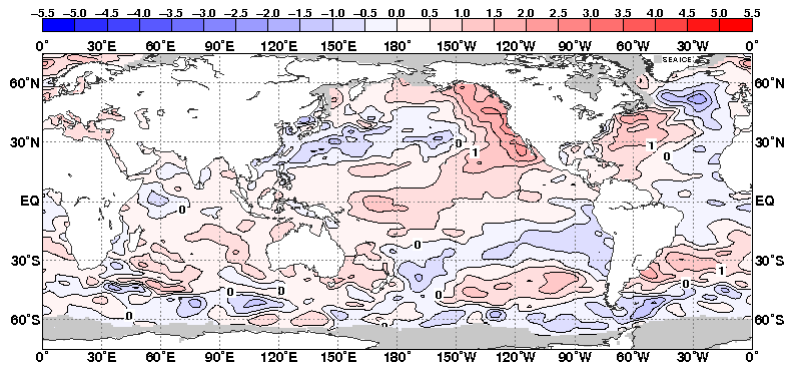


Figure 2.1 Three-month mean sea surface temperature (SST) anomalies for December 2014 – February 2015
The contour interval is 0.5°C.

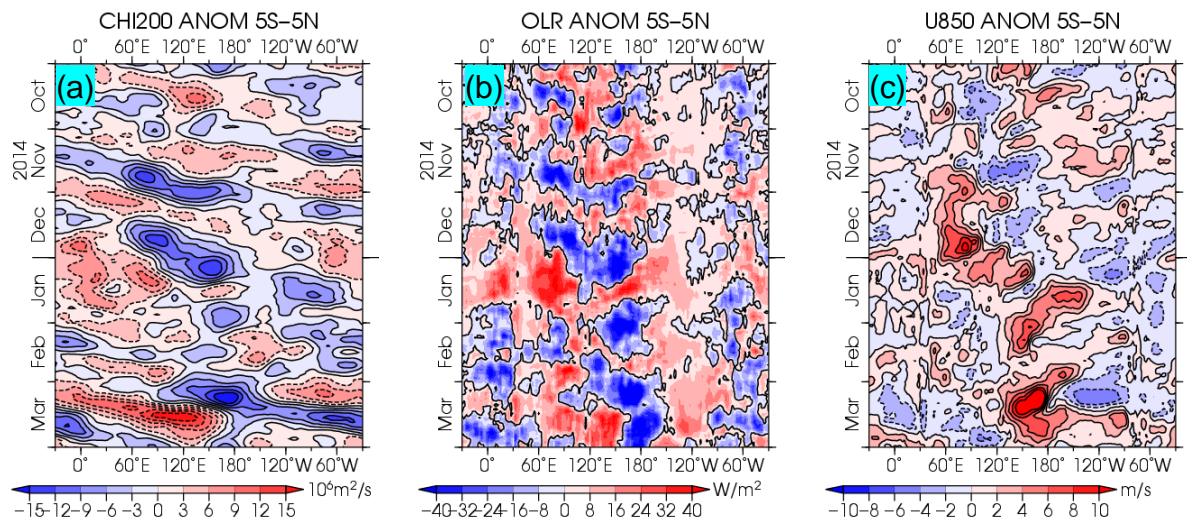


Figure 2.2 Time-longitude cross section of seven-day running mean (a) 200-hPa velocity potential anomalies, (b) outgoing longwave radiation (OLR) anomalies, and (c) 850-hPa zonal wind anomalies around the equator (5°S – 5°N) from October 2014 to March 2015

(a) The blue and red shading indicate areas of divergence and convergence anomalies, respectively. (b) The blue and red shading indicate areas of enhanced and suppressed convective activity, respectively. (c) The blue and red shading show easterly and westerly wind anomalies, respectively.

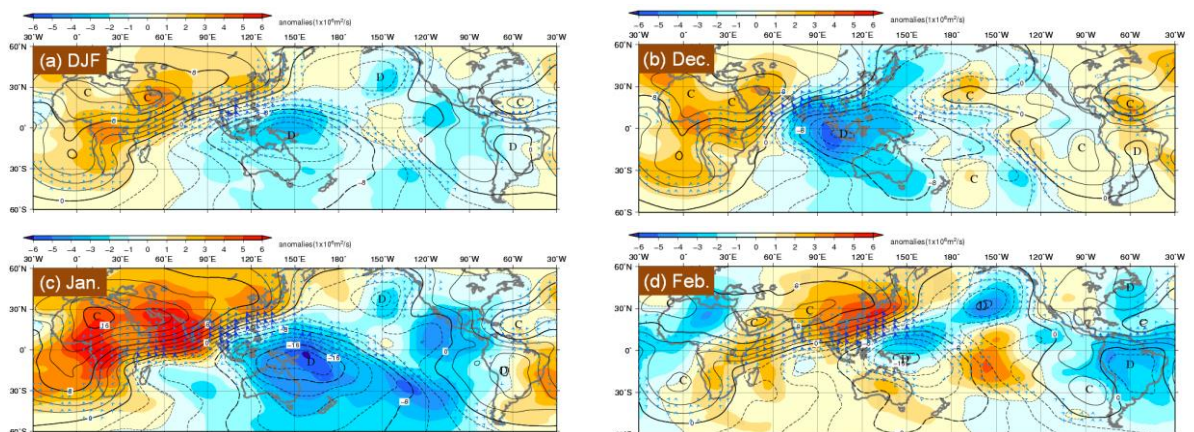


Figure 2.3 200-hPa velocity potential (a) averaged over the three months from December 2014 to February 2015, for (b) December 2014, (c) January 2015 and (d) February 2015

The contours indicate velocity potential at intervals of $2 \times 10^6 \text{ m}^2/\text{s}$, and the shading shows velocity potential anomalies. D and C indicates the bottom and peak of velocity potential, corresponding to the centers of large-scale divergence and convergence, respectively.

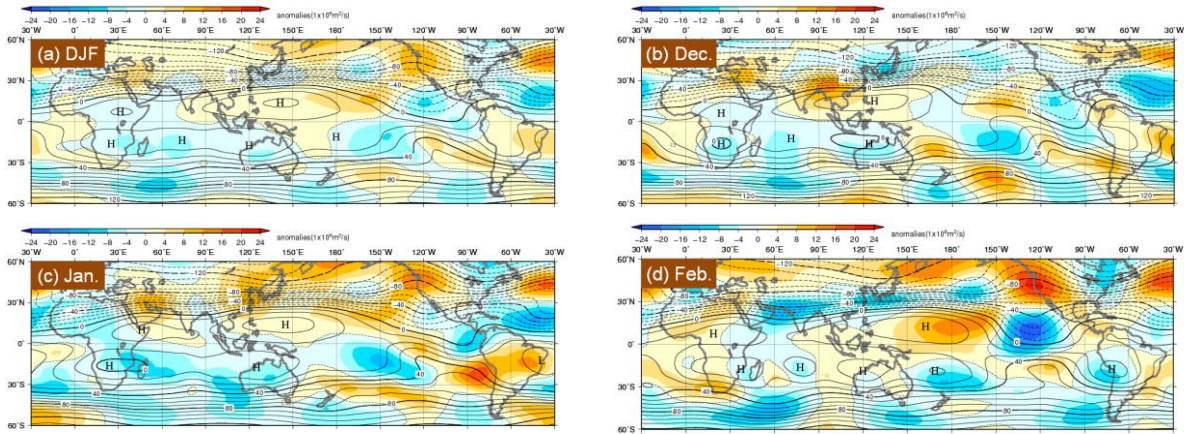


Figure 2.4 200-hPa stream function (a) averaged over the three months from December 2014 to February 2015, for (b) December 2014, (c) January 2015, and (d) February 2015. The contours indicate stream function at intervals of $10 \times 10^6 \text{ m}^2/\text{s}$ and the shadings indicate anomalies. H and L denote the centers of anticyclonic and cyclonic circulation anomalies, respectively.

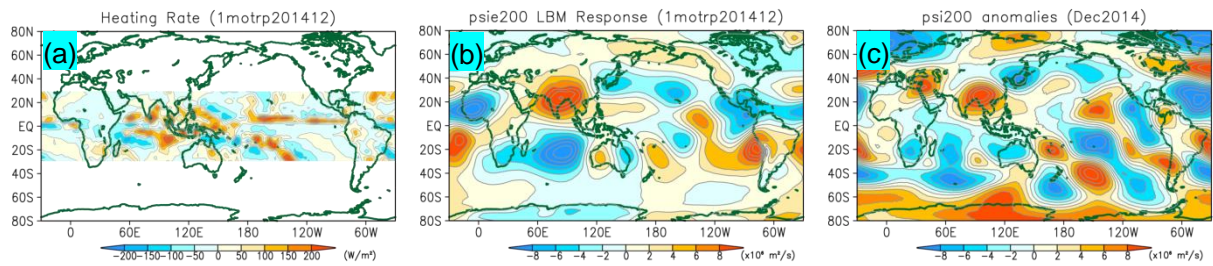


Figure 2.5 Steady response in a linear baroclinic model (LBM) to heating anomalies in the tropics for December 2014. (a) The red and blue shading indicates diabatic heating and cooling anomalies, respectively, for the LBM with the basic state for December (i.e., the 1981 – 2010 average). (b) The shading denotes the steady response of 200-hPa stream function anomalies (m^2/s). (c) The shading shows the actual 200-hPa stream function anomalies for December 2014. The anomalies in (b) represent deviations from the basic states, and are additionally subtracted from the zonal averages of the anomalies.

2.2 Conditions in the extratropics and Asian Winter Monsoon

In winter 2014/2015, the polar vortex tended to shift toward northeastern Canada in the 500-hPa height field (Figure 2.6(a)). In association with distinct ridges persistent over the western part of North America (Figure 2.6(a)), precipitation in the southwestern USA was below normal except December, exacerbating the exceptionally dry conditions that have been around since 2013. As seen in the 500-hPa height field and the sea level pressure field, positive anomalies were persistent in the northern part of the North Atlantic throughout the winter (Figure 2.6 and 2.8) and repeatedly served as a source of wave activity propagating eastward through Europe towards East Asia. The intensity of the Siberian High varied throughout the winter with being stronger than normal in the first half of December and from late January to early February and weaker than normal from late December to mid-January and in mid-February (Figure 2.9 (a)). The intensity averaged throughout the winter was close to normal (Figure 2.9(b)).

In December 2014, a dipole-type blocking developed over East Siberia (Figure 2.6 (b)). A wave-train pattern was noticeable along the polar front jet stream from the Atlantic Ocean eastward, indicating a contribution to negative height anomalies and cold temperatures in East Asia.

In February 2015, an overall pattern with negative anomalies in the Arctic and positive anomalies in mid-latitudes was seen in the 500-hPa height field, associated with a positive phase of Arctic Oscillation. Parts of the area from Eastern Siberia to northern Japan experienced extremely high temperatures, likely attributable to the weaker-than-normal Siberian High and a blocking-like ridge that developed around the Kamchatka Peninsula (Figure 2.6(d)).

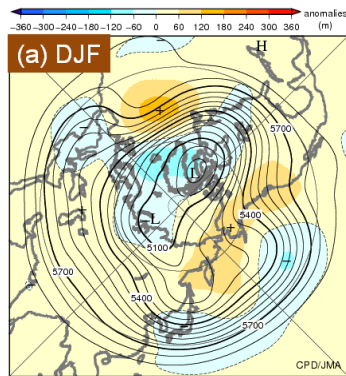


Figure 2.6 500-hPa height (a) averaged over the three months from December 2014 to February 2015, for (b) December 2014, (c) January 2015, and (d) February 2015

The contours indicate 500-hPa height at intervals of 60 m, and the shading denotes anomalies. H and L indicate the peak and bottom of 500-hPa height, respectively, and + (plus) and - (minus) show the peak and bottom of anomalies, respectively.

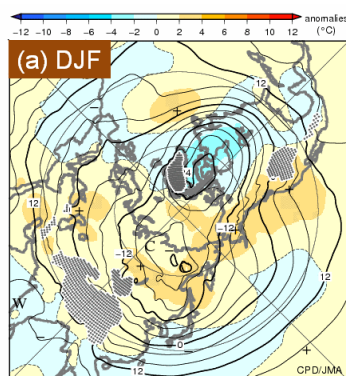
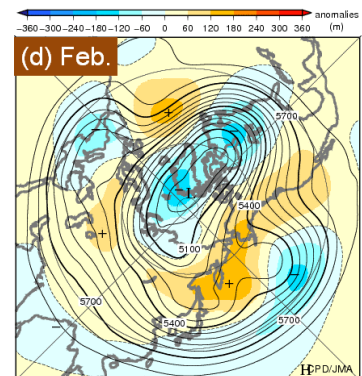
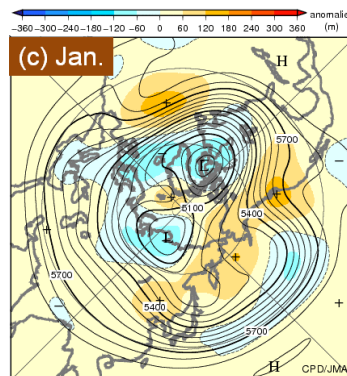
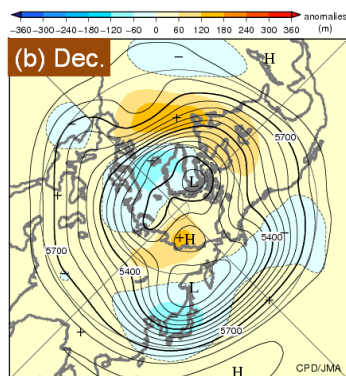
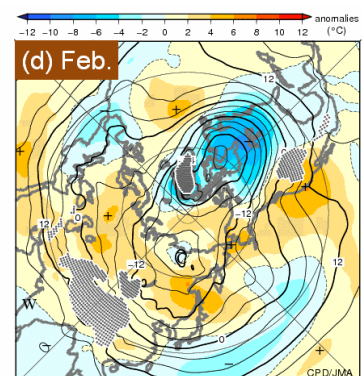
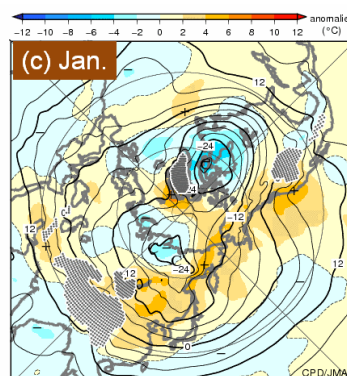
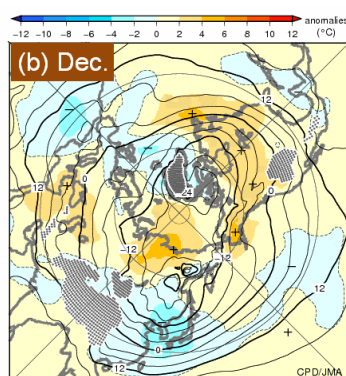


Figure 2.7 850-hPa temperature (a) averaged over the three months from December 2014 to February 2015, for (b) December 2014, (c) January 2015, and (d) February 2015

The contours indicate 850-hPa temperature at intervals of 4°C, and the shading denotes anomalies. W and C indicate the centers of warm and cold air, respectively, and + (plus) and - (minus) show the peak and bottom of 850hPa temperature anomalies, respectively.



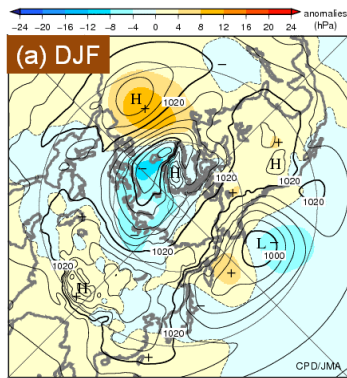


Figure 2.8 Sea level pressure (a) averaged over the three months from December 2014 to February 2015, for (b) December 2014, (c) January 2015 and (d) February 2015

The contours indicate sea level pressure at intervals of 4 hPa, and the shading shows related anomalies. H and L indicate the centers of high and low pressure systems, respectively, and + (plus) and - (minus) show the peak and bottom of sea level pressure anomalies, respectively.

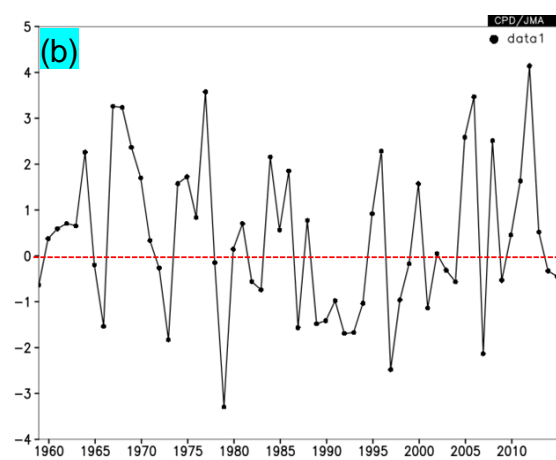
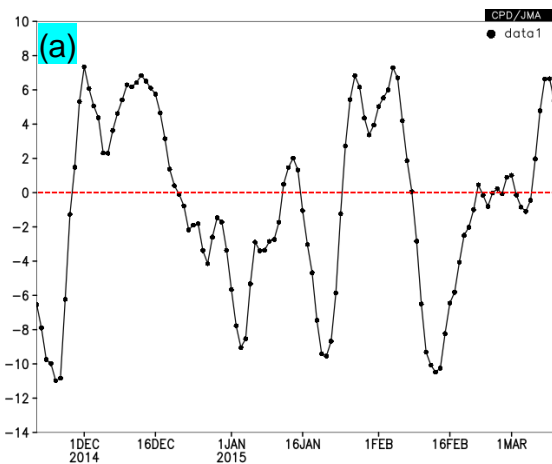
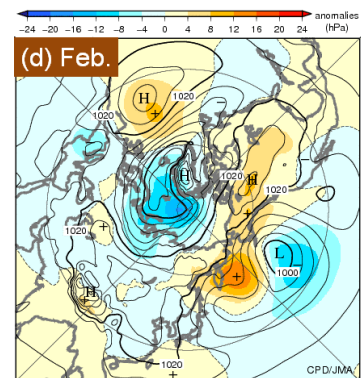
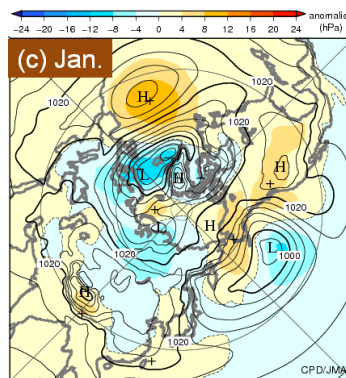
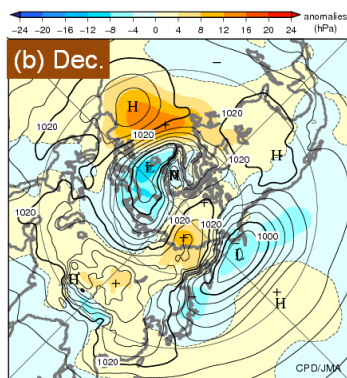


Figure 2.9 (a) Intraseasonal and (b) interannual variations of area-averaged sea level pressure anomalies around the center of the Siberian High ($40^{\circ}\text{N} - 60^{\circ}\text{N}, 80^{\circ}\text{E} - 120^{\circ}\text{E}$) for winter

(a) The black line indicates five-day running mean values from 21 November 2014 to 10 March 2015. (b) The black line indicates three-month mean values for winter from 1958/1959 to 2014/2015.

References

- JMA, 2006: Characteristics of Global Sea Surface Temperature Data (COBE-SST), *Monthly Report on Climate System*, Separated Volume No. 12.
- Kobayashi, S., Y. Ota, Y. Harada, A. Ebata, M. Moriya, H. Onoda, K. Onogi, H. Kamahori, C. Kobayashi, H. Endo, K. Miyaoka, and K. Takahashi, 2015: The JRA-55 Reanalysis: General Specifications and Basic Characteristics. *J. Meteorol. Soc. Japan*, **93**, 5 – 48.